Application of Nocilla Model for Plume Impingement Analysis

Gennady N. Markelov

AOES Group BV, Haagse Schouwweg 6G, 2332 KG, Leiden, Netherlands

Abstract. A gas/surface interaction model is very important for prediction of spacecraft aerothermodynamics in free-molecular flow, which often occurs in plume impingement onto spacecraft surfaces. A few versions of the Nocilla model: TsAGI, Cook&Hoffbauer, and combined variants; are applied to model a moderate velocity flow past a flat plate and plume impingement for the Aeolus spacecraft. Using a flat plate allows one to compare the versions in details, particularly, to show that information on heat transfer and/or mass flux distribution of scattered molecules are vital to define the Nocilla model parameters properly.

Keywords: gas/surface interaction, Nocilla model, moderate velocity, a flat plate, plume impingement
PACS: 34.50.Dy

INTRODUCTION

Molecular collisions with spacecraft surfaces play a dominant role in free-molecular flow. Therefore, the accuracy of numerical prediction of spacecraft aerothermodynamics strongly depends on the gas/surface interaction model used. For example, the application of diffuse reflection and Nocilla [1] models for gas/surface interaction leads to very different configurations (positions of solar arrays) of the space station Mir to provide required properties during the initial part of its decent trajectory [2]. Many experimental and theoretical studies have been dedicated to determine the parameters of gas/surface interaction for orbital flight conditions and materials used in spacecraft design. Numerical modeling, such as the direct simulation Monte Carlo (DSMC) method [3], requires a knowledge of the velocity distribution function for scattered molecules. A few models: diffuse/specular, Cercignani-Lampis-Lord [4], and Nocilla; have been developed for use with particle methods. The latter has received quite a lot of attention and many researches have obtained parameters for the model. As a result, many versions exist for high velocities typical of orbital conditions ([5, 6], and references herein).

A gas/surface interaction model is also very important for a plume impingement analysis. This is because flow is in near free-molecular regime in the back portion of the plume and at large distances from a thruster, for example, in the case of direct impingement onto spacecraft solar array. Species composition and kinetic energy of molecules exhausted from chemical thrusters significantly differ from corresponding values at low Earth orbit. This has necessitated another series of measurements of molecular beam interaction with a flat plate covered by materials, which are in use in the space industry [7]. Chemical species were CO, CO2, N2, and H2 and molecular beam velocity was varied in the range of 1.6-4.1 km/sec. Based on these experimental data, another version of the Nocilla model has been proposed [8], however, the model has never been applied for numerical analysis.

The objectives of the paper are to compare different versions of the Nocilla model for moderate-velocity free-molecular flow past a flat plate and then to apply them for three-dimensional computations of plume impingement for Aeolus spacecraft.

THRUSTERS, AEOLUS GEOMETRY, AND PLUME PROPERTIES

The propulsion system of the Aeolus spacecraft is based on ARC MONARC 5 N thrusters that have a bell nozzle profile with throat and exit diameters of 1.98 mm and 23.1 mm, respectively [9]. The thruster can operate at different chamber pressures, and in the present paper, chamber pressure and temperature are equal to 8.3 bar and 700° C, respectively. The dissociation of ammonia is about 50-70% depending on the chamber properties. However, in this paper, almost complete dissociation is applied. This is because it simplifies the numerical analysis (only two major species, H_2 and N_2) and does not change the conclusions. Four pairs of thrusters are located in the vicinity of $-X$ side of the spacecraft box. Figure 1 shows the thruster positions and densities in three cross-sections and heat fluxes, over Aeolus surface, in the case of four thrusters firing. For plume impingement analysis, only half of the Aeolus geometry with deployed solar panels in $-X$ direction is considered. The spacecraft surface is covered by different materials. For

simplicity, it is assumed here that the face side of the Aeolus solar panels is covered by glass and that white enamel covers the rest of the spacecraft. To compute disturbing forces and torques, the following coordinate system is used. The Z-axis is the vertical centerline of the spacecraft, with the bottom of the spacecraft box at Z=0.2 m. The $-X$ axis is colinear with the solar array centerline. The center of gravity is at the origin of the coordinate system.

The Navier-Stokes solver, CFD-FASTRAN [10], and DSMC-based software, SMILE [11], were used for computations: a continuum approach in the thruster nozzle and near plume field and a kinetic approach for plume impingement (see details in [9]). The solar panels are located at a large distance from the thrusters and the velocity of hydrogen is almost constant at 2200 m/sec in the vicinity of solar panels centerline. The velocity of nitrogen varies from 1950 to 2100 m/sec with distance from the spacecraft side-wall and the angle of incidence increases from about 48 to 83 deg.

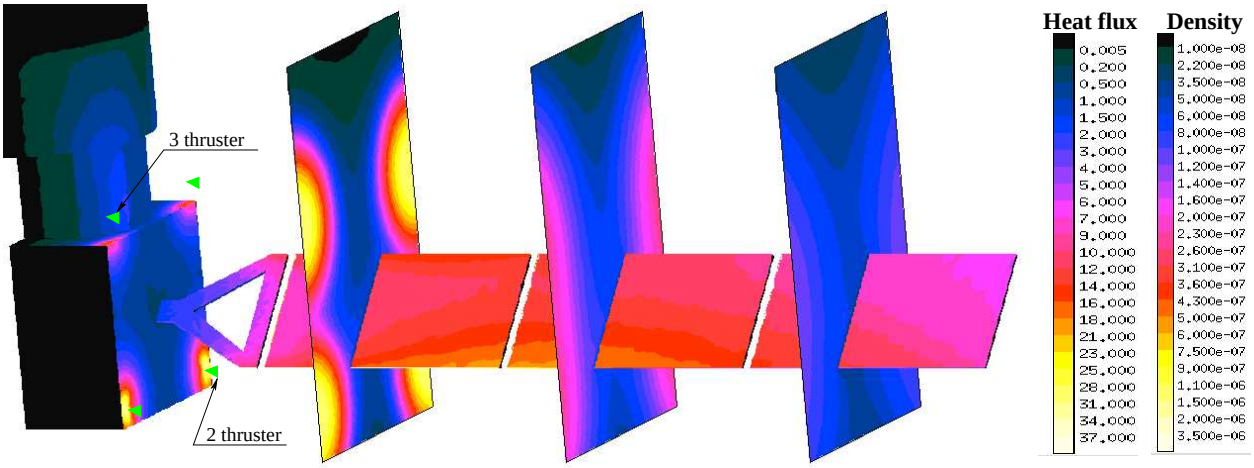

FIGURE 1. Convective heat fluxes (values in W/m^2) over Aeolus surface and density flowfield (values in kg/m^3), $T_w = 273$ K

NOCILLA MODEL

Nocilla [1] has suggested that a distribution function of scattered molecules can be represented by a Maxwellian distribution with a drifted velocity. The model has five parameters: density, temperature, and three components of velocity. An equality of incident and scattered fluxes defines the density, and one of the velocity components can be removed by a proper choice of coordinate system. For example, a component of velocity perpendicular to a plane, determined by a velocity vector of an incident molecule and surface normal, is zero. The other three free parameters are obtained using experimental data and/or introducing assumptions [12, 6, 8]. The following subsections give a brief description of several ways of determining the Nocilla model parameters. For the sake of simplicity, they are hereafter referred to as models. The reader, interested in the formulae, should consult Refs. [9, 12, 8].

TsAGI model

To determine the parameters of the Nocilla model, TsAGI has conducted a great many experiments on interactions of molecular beams with engineering surfaces, typical for space applications [5, 12]. Beam velocities were varied from 4 up to 8 km/sec and molecules were N_2 and/or O_2. Forces exerted on surfaces and angular distribution of scattered molecules, were measured and approximations were obtained for normal and tangential forces and normal component of speed ratios vs angles of incidence. The TsAGI model has been applied extensively to calculate aerodynamic characteristics of spacecraft at LEO. The model does not require an iterative process and it is very efficient for numerical modeling.

Cook & Hoffbauer (CH) model

The interaction of molecular beams of moderate velocity (1.6 up to 4.1 km/sec) and chemical species typical for plume thruster flows (H_2, N_2, CO, CO_2) with a flat plate, was studied by S. Cook [7]. Forces exerted on surfaces of Kapton, SiO2-coated Kapton, solar array material, and white paint Z-93 were measured and Ref. [8] proposed an alternative way to determine the parameters of the Nocilla model. The forces are defined by reduced force coefficients, obtained from experimental data. To determine the last free parameter, it is assumed that accommodation coefficients of kinetic energy, defined for averaged squared velocities and squares of averaged velocities, are equal. Using the

equations for forces and energy flux, a nonlinear equation for normal component of a speed ratio can be derived (see [9]). The forces were measured only at room temperature, $T_w = 295$ K, and for two values of incidence velocity. Normal force coefficients depend on incident velocity, except for the solar array material [7] and so it was suggested to use linear interpolation to find the values of reduced coefficients for a particular velocity.

Figure 2 shows reduced coefficients obtained from the TsAGI model and by experiments [7]. The TsAGI model gives a normal force coefficient close to Cook's data, the difference is about 10% which is an uncertainty of the experimental data. Despite the fact that TsAGI performed measurements for N_2 and O_2 only, the model also predicts a normal force coefficient for H_2 very well. The coefficient is slightly above that of Cook's data. The TsAGI prediction of the tangential force coefficient agrees well with the data [7] up to an angle of 40 deg, but beyond this value they deviate. Angular distributions of scattered molecules obtained with the TsAGI and CH models are very different for N_2 and this difference increases with incidence angle (Fig 2, right). The difference is significantly less for H_2 and correspondent angular distributions are shown in [9].

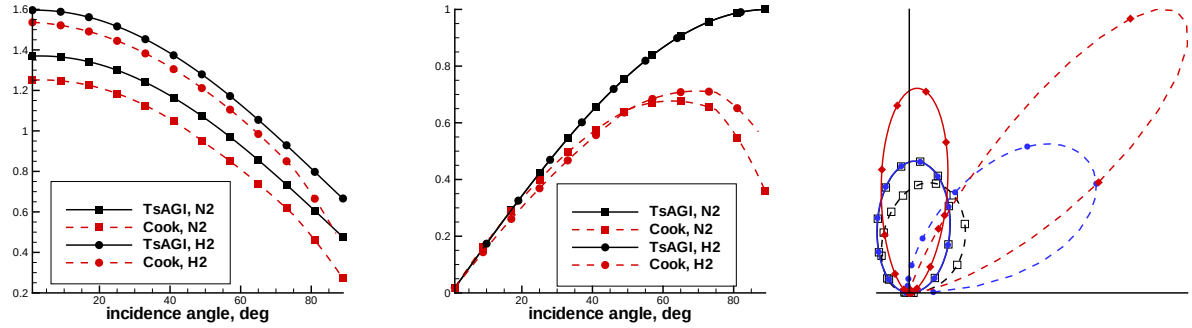

FIGURE 2. Reduced normal (left) and tangential (middle) force coefficients for TsAGI model and Cook data for solar array material ($T_w = 295$ K, $v_i = 1870$ and 2590 m/sec for N_2 and H_2, respectively); right, angular density distributions for solar array material: square, TsAGI; diamond, CH; circle, combined model; solid, $\theta_i = 25$ deg; dashed, $\theta_i = 85$; $T_w = 295$ K, N_2, $v_i = 1870$ m/sec

Combined model

Ref. [9] has used a model that combines the TsAGI and CH models, which is based on the TsAGI approximation for the normal component of the speed ratio. Because the equation is based on measurements of mass flux distribution of scattered molecules, avoids an iterative process. The other two equations are based on experimental data [7]. The tangential reduced force is calculated exactly as in the CH model, whereas the normal force is determined by the modified normal force coefficients. These do not depend on incident velocity and allow wall temperatures to be taken into account. Values of the reduced force coefficients between experimental points are interpolated with second-order polynomials.

The model predicts exactly the same forces as the CH model but different angular distribution of scattered molecules. For small angles of incidence, the model predicts angular distributions of N_2 close to the TsAGI model and for larger angles the combined model predictions are closer still (see Fig. 2, right). The situation is opposite for H_2 distributions, for which the combined model gives distributions very similar to results from the CH model.

FREE-MOLECULAR FLOW OVER A FLAT PLATE

The above-mentioned models have been applied to compute a free-molecular flow past a flat plate. Two surface materials are considered: glass and white enamel for the TsAGI model and solar material and white paint Z93 for the CH/Combined models. In addition, computations have been performed with a diffuse reflection with complete energy accommodation. Free-stream flow properties correspond to experimental conditions [7] and plume flow properties to those along Aeolus solar array centerline. The wall temperature is 295 and 273 K for experimental and Aeolus conditions, respectively.

Experimental conditions

Figure 3 show axial, C_X, and normal, C_Y, force coefficients and lift-to-drag ratio, K, for N_2 molecular beam. For glass/solar array material, the Nocilla model predicts smaller axial force and higher normal force, especially, in the

case of the TsAGI model than diffuse reflection. The lift-to-drag ratio vs angle of incidence is almost a straight-line for the TsAGI model, whereas the CH model gives a higher value at large incidence angle. For white enamel/paint, the CH model predicts a lower lift-to-drag ratio than the TsAGI model. Moreover, molecules backscatter for the CH model for angle $\theta_i > 80$ deg because the Z93-coated surface was found to be rough on a 100-micron scale. That leads to the horizontal part of the lift-to-drag dependence. The TsAGI model provides the lowest heat transfer coefficient, C_h, over other models. Heat transfer coefficients for the CH model almost coincide with those from diffuse reflection. The Combined model gives values that are close to those of the CH model.

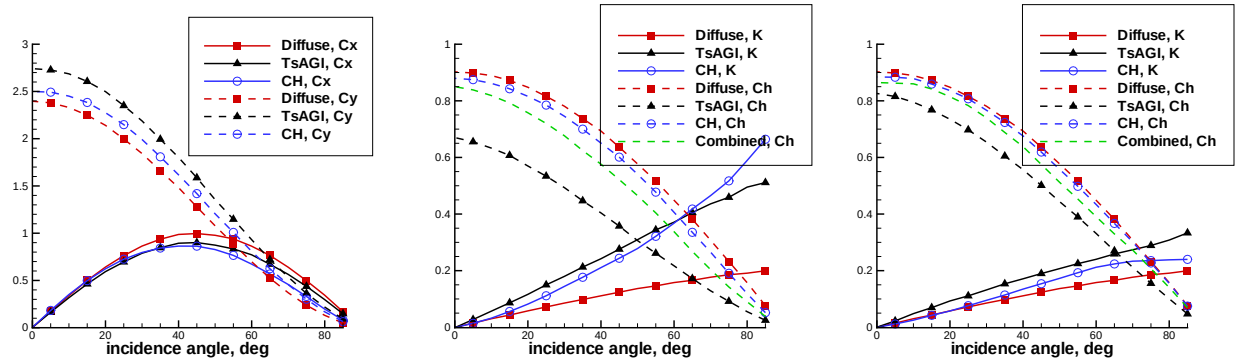

FIGURE 3. Axial, C_x, and normal, C_y, forces and heat transfer, C_h, coefficients and lift-to-drag ratio, K, for N_2, v_i=1870 m/sec, $T_w = 295$ K (left and middle, glass/solar array material; right, white enamel/paint)

The application of these models for hydrogen flow gives similar effects on forces and the lift-to-drag ratio (Fig. 4). Now the CH model predicts slightly smaller lift-to-drag ratio than the TsAGI model for the considered range of angles of incidence and the CH model results show a rather small horizontal part for white paint material. Concerning heat transfer coefficients, the CH prediction is in very good agreement with diffuse reflection results. The TsAGI model predicts negative values for the majority of incidence angles. Note the model was not developed for hydrogen molecules or moderate velocities. The Combined model is based on the TsAGI approximation of normal component of speed ratio and this model provides the same qualitative behavior of heat transfer as the TsAGI model except that the values are more positive. For white paint, the Combined model predicts higher values of heat transfer than the CH model and diffuse reflection for angles of incidence are less than 40 deg. An intuitive solution, scaling of the normal component of the speed ratio with $\sqrt{m_{H_2}/m_{N_2}}$, decreases the variation of the heat transfer coefficient but preserves the qualitative dependence and values higher than diffuse reflection results. Obviously, experimental data on heat transfer and/or mass flux distribution of scattered molecules are vital to validate gas/surface interaction models.

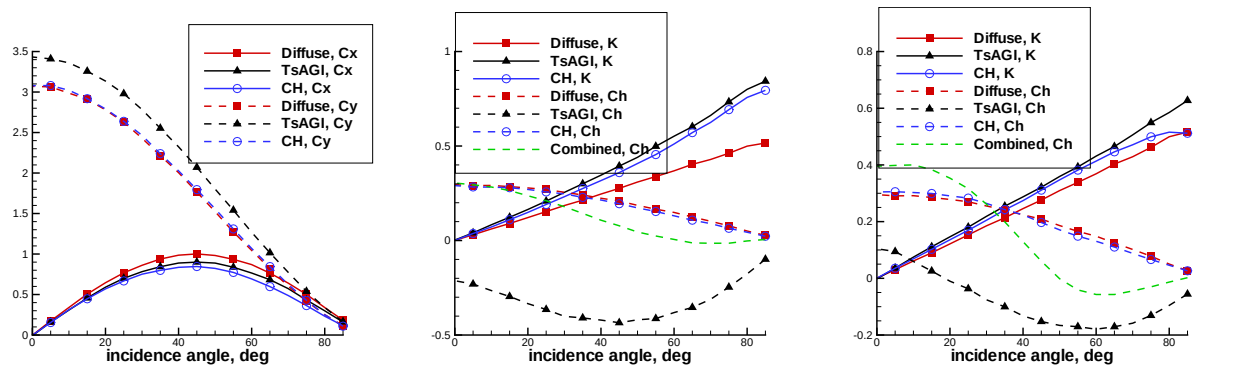

FIGURE 4. Axial, C_x, and normal, C_y, forces and heat transfer, C_h, coefficients and lift-to-drag ratio, K, for H_2, v_i=2590 m/sec, $T_w = 295$ K (left and middle, glass/solar array material; right, white enamel/paint)

Aeolus plume conditions

This section presents the results for a flat plate when the free-stream flow corresponds to the undisturbed plume properties near a solar array centerline. Computations are performed for face and back sides of the solar array. Force

and heat transfer coefficients gradually decrease with distance from the spacecraft body (Fig. 5). This is because the angle of incidence increases from 48 deg at a leading edge of the first solar panel, up to 83 deg at the trailing edge of the third solar panel. The Nocilla model predicts a smaller axial force and higher normal force than diffuse reflection for glass/solar array materials. For white enamel/paint, all models give very similar results, because molecules scatter almost diffusively from this surface material. The heat transfer coefficient is positive for the TsAGI and Combined models along an entire centerline, because the hydrogen mass fraction is about 10%. However, for glass/solar array material, the TsAGI model gives a very negative heat flux for hydrogen (see Fig. 4, middle) and the difference between model predictions is almost a factor of 3 for the face side of the solar array.

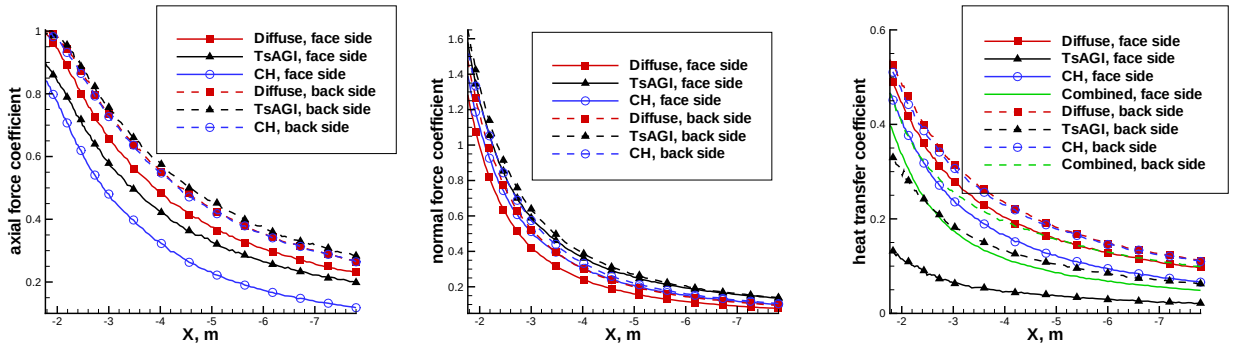

FIGURE 5. Forces and heat transfer coefficients along solar array centerline (Aeolus plume conditions, $T_w = 273$ K)

PLUME IMPINGEMENT

3D computations of plume impingement have been performed with SMILE software for four thrusters firing independently and altogether. This section presents results obtained for the second and third thrusters only. Plumes exhausted from these thrusters impinge on face and back sides of the solar panels, respectively, and produce the largest forces and torque. An application of different gas/surface interaction models changes forces similar to the behavior shown in the previous section. The CH/Combined model provides the smallest absolute F_X for the face side of the solar array, which is only about 60% of the diffuse reflection result. Maximum absolute values of F_Y and F_Z are predicted by the TsAGI model. Obviously a difference in model predictions is smaller for back side of the solar panels. Torques are the cross product of forces and their offsets. However, for the considered geometry, they also follow the dependence of normal force for a flat plate. Namely, the TsAGI model predicts the highest absolute values and the CH model gives values that are between those of the TsAGI and diffuse model results. The Combined model gives the same results as the CH model.

TABLE 1. Forces and torques ($T_w = 273$ K, F_T is a thruster thrust, $M = F_T \times 1m$)

model	thruster	F_X/F_T, %	F_Y/F_T, %	F_Z/F_T, %	M_X/M, %	M_Y/M, %	M_Z/M, %
diffuse	2	-1.5897	0.8673	0.8827	-0.9095	1.6359	-3.3378
diffuse	3	-1.3632	-0.7139	-0.8303	0.6330	-4.4398	2.8514
TsAGI	2	-1.4338	1.1296	1.1599	-1.1864	2.9524	-4.4211
TsAGI	3	-1.3072	-0.8869	-0.9893	0.7961	-5.1161	3.5852
CH	2	-1.1170	0.9457	0.9774	-0.9978	2.4902	-3.6237
CH	3	-1.3521	-0.7627	-0.8676	0.6875	-4.6030	3.0299
Combined	2	-1.1177	0.9449	0.9775	-0.9970	2.4907	-3.6214
Combined	3	-1.3507	-0.7591	-0.8643	0.6837	-4.5841	3.1403

Heat fluxes are the main concern of the Aeolus project and consequently the thruster centerlines are tilted by 15 deg from $-X$ axis in XY plane. As a result, the plume interacts heavily with the solar panel edge nearest to the plume centerline. For example, heat fluxes vary by a factor of 3 in transversal direction over a solar panel surface and maximum heat fluxes for both sides occur at the edges for the second and third solar panels (Table 2). Diffuse reflection provides the highest heat fluxes and the lowest are obtained with the TsAGI model. A difference between these model results is about a factor of 2 to 3, except for the edge of the third solar panel, for which a maximum heat flux is observed on a leading edge, due to a direct plume impingement. The CH and Combined models give similar

values, except for the face side of the third solar panel. A plausible reason is that the flow is not completely free-molecular and that inter-molecular collisions affect plume properties for different scattering laws (see Fig. 2, right). It seems there is a contradiction with the results of forces and torque, which are equal for both models. There was no difference, because the forces were created due to plume interaction mainly with the first solar panel and different angular distributions of scattered molecules do not have significant effect, due to the small number of inter-molecular collisions. The second and third solar panels are located downstream and so effect of molecular collisions becomes more important. For back side covered by white paint, molecules scatter almost diffusively and the difference in these model predictions is small. The CH model prediction is higher and close to those of diffuse reflection values, as it was obtained for a flat plate case.

TABLE 2. Maximum convective heat fluxes (values in W/m^2, $T_w = 273$ K)

model	thruster	1st solar panel			2nd solar panel			3rd solar panel		
		front	back	edge	front	back	edge	front	back	edge
Diffuse	2	18.99	0.00	11.32	18.93	0.00	53.53	12.12	0.01	43.12
Diffuse	3	0.00	12.20	4.95	0.00	12.95	30.90	0.00	10.92	37.99
TsAGI	2	5.09	0.00	7.22	5.18	0.00	49.46	3.31	0.00	43.71
TsAGI	3	0.00	6.40	2.66	0.00	6.91	26.74	0.00	5.97	36.15
CH	2	10.66	0.00	10.60	9.68	0.00	58.66	3.98	0.00	49.74
CH	3	0.00	10.85	4.38	0.00	11.94	31.54	0.00	10.54	39.09
Combined	2	11.07	0.00	9.83	10.81	0.00	58.43	6.58	0.00	49.57
Combined	3	0.00	9.69	3.92	0.00	11.02	31.16	0.00	9.74	39.83

CONCLUSIONS

Versions of Nocilla model (TsAGI, Cook&Hoffbauer (CH), Combined) are applied to compute the plume impingement on the solar array of the Aeolus spacecraft. The flow near the solar array is near free-molecular and gas/surface interaction is very important for an accurate prediction of forces, torques, and heat fluxes. The models are compared in detail for a simple test case: a flat plate. The comparison reveals that the TsAGI model is accurate for nitrogen flow, even for moderate velocity, however, a straightforward application of the model to hydrogen flow produces negative heat fluxes.

Plume impingement is characterized by low velocity and chemical composition differs from a flow on orbit. Therefore, gas/surface interaction models have to be based on corresponding measurements and theoretical studies. The CH model is based on such experimental data for forces but an additional assumption is required to define all parameters of the Nocilla model. The assumption, an equality of kinetic energy accommodation coefficients, leads to the following. The model predicts heat fluxes that are very close to corresponding values obtained by diffuse reflection with complete energy accommodation. The importance of this assumption for plume impingement analysis is shown by application of the Combined model, which utilizes experimental data [7] and the TsAGI approximation for normal component of speed ratio. This model provides the same forces as the CH model, but different heat fluxes and angular distribution of scattered molecules. Experimental data on heat transfer coefficient and/or mass flux distribution of scattered molecules are vital for the validation and design of appropriate models for plume impingement modeling.

REFERENCES

1. Nocilla S. The surface re-emission law in free molecule flow, Proc. of the III Int. Symp. on RGD, Vol. 1, 1963, pp. 327-346.
2. G. N. Markelov, A. V. Kashkovsky, and M. S. Ivanov, Journal of Spacecraft and Rockets, Vol. 38, No. 1, 2001, pp. 43-50.
3. G. A. Bird, *Molecular Gas Dynamics and the Direct Simulation of Gas Flows*, Pergamon Pres., 1994.
4. R. G. Lord, Physics of Fluids, Vol. 7, No. 5, 1995, pp. 1159-1161.
5. S. V. Musanov, A. P. Nikiforov, A. L. Omelik, O. G. Freedlender, in Proc. of XIII Int.Symp. on RGD, Plenum, New York, Vol. 1, 1985, pp. 669-676.
6. F. G. Collins, and E. C. Knox, AIAA Journal, Vol. 32, pp. 765-773, 1994.
7. S. R. Cook, Ph.D. thesis, the University of Texas at Austin, 1995.
8. S. R. Cook, and M. A. Hoffbauer, Journal of Spacecraft and Rockets, Vol. 34, No. 3, 1997, pp. 379-383.
9. G. N. Markelov, Numerical Analysis of Plume Impingement for Aeolus Spacecraft, AIAA Paper 2005-5067, 2005.
10. CFD-FASTRAN manual, ESI US R&D Inc., 2004.
11. M. S. Ivanov, G. N. Markelov, S. F. Gimelshein, AIAA Paper 98-2669, 1998.
12. O. G. Freedlender, A. P. Nikiforov, in Proc. of 2nd Int.Symp. on Envir. Testing for Space Programmes, ESA WPP-066, 1993.